Defence Research and Development Canada | Recherche et développement pour la défense Canada

CAN UNCLASSIFIED

DRDC | RDDC
technologysciencetechnologie

Multi-period Coverage Path Planning and Scheduling for Airborne Surveillance

Yinghui Wang, Thiagalingam Kirubarajan, Ratnasingham Tharmarasa

McMaster University,

Rahim Jassemi-Zargani and Nathan Kashyap

DRDC – Centre for Operational Research and Analysis

IEEE Transactions on Aerospace and Electronic Systems

Date of Publication from Ext Publisher: March 2018

Defence Research and Development Canada

External Literature (P)

DRDC-RDDC-2018-P106

August 2018

Canada

IMPORTANT INFORMATIVE STATEMENTS

This document was reviewed for Controlled Goods by Defence Research and Development Canada (DRDC) using the Schedule to the *Defence Production Act*.

Disclaimer: This document is not published by the Editorial Office of Defence Research and Development Canada, an agency of the Department of National Defence of Canada but is to be catalogued in the Canadian Defence Information System (CANDIS), the national repository for Defence S&T documents. Her Majesty the Queen in Right of Canada (Department of National Defence) makes no representations or warranties, expressed or implied, of any kind whatsoever, and assumes no liability for the accuracy, reliability, completeness, currency or usefulness of any information, product, process or material included in this document. Nothing in this document should be interpreted as an endorsement for the specific use of any tool, technique or process examined in it. Any reliance on, or use of, any information, product, process or material included in this document is at the sole risk of the person so using it or relying on it. Canada does not assume any liability in respect of any damages or losses arising out of or in connection with the use of, or reliance on, any information, product, process or material included in this document.

© Her Majesty the Queen in Right of Canada (Department of National Defence), 2018

© Sa Majesté la Reine en droit du Canada (Ministère de la Défense nationale), 2018

This article has been accepted for publication in a future issue of this journal, but has not been fully edited. Content may change prior to final publication. Citation information: DOI 10.1109/TAES.2018.2812538, IEEE Transactions on Aerospace and Electronic Systems

Multi-period Coverage Path Planning and Scheduling for Airborne Surveillance

Yinghui Wang, T. Kirubarajan and R. Tharmarasa
McMaster University, Hamilton, ON, Canada
Rahim Jassemi-Zargani and Nathan Kashyap
Defence Research and Development Canada Ottawa Research Centre, Ottawa, ON, Canada

***Abstract*—In this paper, optimal surveillance mission plans are developed to cover disjoint areas of interest (AOIs) over an extended time horizon using multiple aerial vehicles. AOIs to be covered are divided into a number of cells. To promptly update information collected from AOIs and to ensure persistent surveillance, each cell is to be revisited within a time slot. Joint path planning and temporal scheduling is formulated as a combinatorial optimization with the proposal of novel objective functions: 1) maximizing the minimum number of non-repeatedly covered cells in a sliding-window fashion and 2) maximizing the total number of covered cells in the mission plan. A multi-objective evolutionary algorithm (MOEA) with a specific chromosome representation and custom genetic operators, in which the constraint that each cell be revisited within a time slot is transformed into the third objective to handle infeasibility, is developed. The initial single-period paths are generated by solving a series of orienteering problems. The initial population is obtained by connecting these single-period paths and selecting the take-off time for each flight. Three mutation moves are proposed to enable revisiting in a single-period path and rescheduling of take-off time. The solutions converge in the MOEA and are selected by a weighted-sum model according to user preferences in decision making. Simulation results on different mission scenarios and different criteria show the superiority of the proposed algorithm. The algorithm is done offline ahead of the missions and requires modest computational resources.**

***Index Terms*—Disjoint area surveillance, Persistent surveillance, Path planning, Temporal scheduling, Multi-objective optimization.**

ACRONYMS

AOI	Area of interest
CPP	Coverage path planning
EA	Evolutionary algorithm
ISR	Intelligence, surveillance and reconnaissance
MOEA	Multi-objective evolutionary algorithm
MOO	Multi-objective optimization
MTZ-SEC	Miller-Tucker-Zemlin subtour elimination constraint
NSGA	Non-dominated sorting genetic algorithm
OP	Orienteering problem
POI	Point of interest
TSP	Travelling salesman problem
UAV	Unmanned aerial vehicle

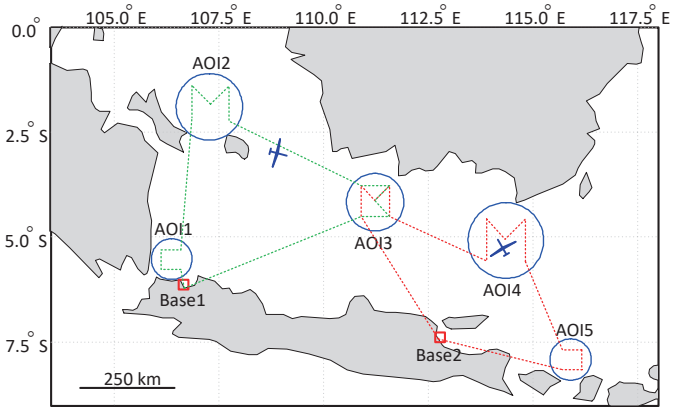

Fig. 1: Mission planning scenario: two aircraft conduct intelligence-gathering over five AOIs.

I. INTRODUCTION

In order to have the capabilities to observe, analyze, record and report activities in disjoint areas of interest (AOIs), it is often necessary to upgrade expensive airborne surveillance systems to maximize effectiveness [19, 23]. Technological advances in manned or unmanned vehicles and modernized sensor sets have enabled patrolling frequency to be increased and surveillance areas expanded. Efficient mission plans have become critical for intelligence, surveillance and reconnaissance (ISR) operations [23].

The purpose of this study is to derive a mission plan for multiple aircraft over an extended time horizon (e.g., 48 hours) in order to maximize the information collected over a number of disjoint AOIs (as shown in Fig. 1). It is required that regions inside AOIs be revisited within a given time slot (e.g., 8-hour slot). The spatio-temporal control of aircraft for a given planning horizon is determined to provide prompt and useful information as well as to achieve persistent and effective surveillance.

Very few studies in coverage path planning (CPP) [4] or path planning using coverage pattern templates [12, 18, 19] have looked at multiple vehicles covering disjoint target regions, which is a common question in surveillance missions. Similar to [19], our problem includes disjoint AOIs, path planning inside AOIs, and aircraft take off from and land at the same base. However, in our study, an AOI can be of any shape and the path inside an AOI does not necessarily follow the

0018-9251 (c) 2018 IEEE. Personal use is permitted, but republication/redistribution requires IEEE permission. See http://www.ieee.org/publications_standards/publications/rights/index.html for more information.

This article has been accepted for publication in a future issue of this journal, but has not been fully edited. Content may change prior to final publication. Citation information: DOI 10.1109/TAES.2018.2812538, IEEE Transactions on Aerospace and Electronic Systems

strips as in [19]. Instead of using coverage pattern templates, paths for one flight are generated by a heuristic approach. In addition, multiple flights for one aircraft in the mission plan are considered because each aircraft may take off and land multiple times within the mission time horizon, which is referred to as multi-period path planning [2, 32].

The shortest path or the minimum-cost vehicle route is always the objective in the travelling salesman problem (TSP), vehicle routing problem (VRP) and their variants [1, 24, 31]. In contrast, in many surveillance mission planning scenarios, the mission duration is given, and the main objective is to maximize the information collected within this fixed time [11, 23]. In this study, we concentrate on information maximization given the mission time. The orienteering problem (OP, also known as the selective TSP) maximizes the total collected score on a path that visits some of the vertices in limited length [34]. However, our problem cannot be solved by the existing approaches in OPs or turning the cost minimization to a reward maximization in VRPs. The main reasons are as follows:

1) Due to the nature of dynamic surveillance environment, new threats may emerge at any time and the objects of suspicion may evade, which requires periodic or aperiodic revisits of AOIs to update information [18]. Aircraft should make full use of their capacity to survey and not be satisfied with visiting AOIs only once. Therefore, revisit of an area by the same or different aircraft should be allowed. However, every vertex is visited at most once and the score of each vertex can be collected by one vehicle at most in OP [32]. In multiple travelling salesman problems (mTSPs) or VRPs, every vertex is visited exactly once [1, 24].

2) In the proposed problem, collecting information requires searching inside AOIs by covering different areas (as shown in Fig. 1), which not only takes time but also requires path planning inside AOIs. Even though service time is needed when the vehicle visits a customer in some variants of VRP [10], path planning is not conducted within this service time.

3) The proposed problem cannot be solved by simultaneously maximizing travel time (the cost of paths) inside AOIs and minimizing travel time outside AOIs, because each region inside AOIs is required to be revisited within a given time slot. The topology of mission scenario and the mission criteria lead to new objectives and constraints (Sections II and III), which further generate new solution techniques (Section IV).

Note that the information collected in this paper is evaluated by the coverage of AOIs [11, 23] rather than by detecting and tracking targets [25]. Paths are planned offline even if there is no target in the AOIs. Online search and tracking is the topic of a separate publication.

A path planning method for a single unmanned aerial vehicle (UAV) is proposed to maximize the information collected (based on images captured by a camera at the bottom of the UAV) from desired regions while avoiding flying over forbidden regions in [11]. A multivehicle team planning approach is described to maximize the target coverage (number of cells scanned in the region of interest) for surveillance missions [23]. In our paper, the sensing model is similar to what is described in [11, 16, 23]. AOIs to be covered are divided into a number of cells. However, we use two objectives to evaluate the information collected: 1) the number of non-repeatedly covered cells in a sliding-window fashion [5] and 2) the total number of covered cells in the mission plan. Maximizing these objectives not only makes full use of aircraft capacity to cover AOIs but also conquers the problem described in [11] that, once an aircraft enters an AOI, it remains inside instead of flying to other AOIs. Moreover, the surveillance scenarios in our study are more realistic and complicated than those in [11, 23].

In this paper, a sequence of cells is selected to generate a path for one flight (namely, a single-period path) that covers these cells in turn. Since aircraft take off and land multiple times in the mission, single-period paths are connected head to tail with a given minimum downtime (corresponding to aircraft maintenance and refueling time) and an adjustable wait time between two flights, by which paths for multiple flights (namely, multi-period paths) are generated. The mission plan is a collection of multi-period paths for all aircraft, in which paths are planned and the take-off time for each flight is determined.

We formulate the proposed problem as a combinatorial optimization. A multi-objective evolutionary algorithm (MOEA) with a specific chromosome representation and custom genetic operators, which not only selects the paths but also determines the take-off time schedule and enables revisiting in each flight, is developed. The constraint that each cell be revisited within a time slot is transformed into an objective in the evolutionary algorithm (EA).

We believe that our path planning and scheduling yields many original contributions.

1) The proposed objective functions provide new evaluation metrics for coverage path planning in surveillance missions, which promptly update information collected from different areas and make full use of aircraft capacity to cover AOIs.

2) The optimization formulation of multi-period path planning and scheduling, which allows revisiting in a single-period path, is first provided. Path selection and take-off time determination are jointly considered. Revisit of cells in single-period paths and scheduling of take-off time are incorporated in the objectives and constraints, which makes the formulation different from the existing ones in VRPs, OPs and CPPs [12, 24, 34].

3) A new chromosome structure is given to represent the mission plan, which integrates the path selection and the take-off time decision so that multi-period path planning and temporal scheduling can be effectively handled in the MOEA. In the EA, the crossover is performed based on the unit (gene segment) of single-period paths rather than the unit of cells. Three custom moves in the mutation operator, namely *Remove*, *Insert* and *Reschedule*, to enable revisit of cells and scheduling of take-off times, are developed. Because of the chromosome structure and the genetic operators, the proposed algorithm differs from the existing ones in VRPs, OPs and CPPs.

4) The proposed algorithm is intelligent not only because the chromosome structure and the custom genetic operators are used, but also because the final solution can be selected from a set of mission plans provided by the multi-objective

0018-9251 (c) 2018 IEEE. Personal use is permitted, but republication/redistribution requires IEEE permission. See http://www.ieee.org/publications_standards/publications/rights/index.html for more information.

This article has been accepted for publication in a future issue of this journal, but has not been fully edited. Content may change prior to final publication. Citation information: DOI 10.1109/TAES.2018.2812538, IEEE Transactions on Aerospace and Electronic Systems

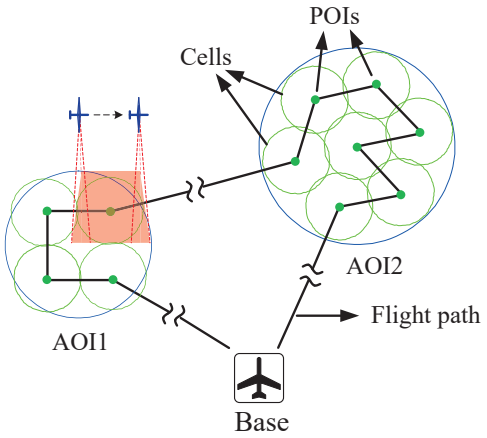

Fig. 2: Illustration of AOIs, cells, POIs, and a flight path.

optimization (MOO) according to the user preferences [8]. The proposed solution framework can be used in a variety of surveillance problems, even though most of the surveillance mission planning problems are application-dependent or environment-dependent [11].

The remainder of the paper is structured as follows. Section II outlines the preliminary information needed to understand the mission scenario and the objectives. Section III presents the formulation of this optimization problem. The solution technique is developed in Section IV. Simulation results are given in Section V. The conclusions are discussed in Section VI.

II. Problem Description

A. Mission Scenario

The geographic AOI can be of any shape, but the geographical and dimensional information about AOIs are known a priori. Each AOI to be searched is divided into a number of cells as shown in Fig. 2. The shape of a cell is determined by the sensor coverage in one scan: for example, the sensing area of an airborne camera facing downward is designed to be a circular region [16] or a rectangular region [11, 18]. Note that a variety of coverage sweep patterns can be used for a cell and that the shape of a cell is not constrained to be circular as shown in Fig. 2 [18, 23]. However, AOI segmentation is not the focus of this paper. The center of a cell is denoted as a point of interest (POI). A cell is considered entirely covered if its center (POI) is visited by an aircraft. In this surveillance problem, we assume that any POI can be visited by at least one aircraft.

The assets consist of a given number of patrolling aircraft. Each aircraft is characterized by its speed of travel, a fixed altitude above ground level, a maximum flight time (constrained by fuel), a minimum and a maximum downtime between two successive flights. The above attributes are given for each aircraft and need not be same for all aircraft. Aircraft with the same speed and the same constraints on flight time and downtime are of the same type. Aircraft are to take off and land from/at the same base station, as shown in Fig. 1 and Fig. 2. It is assumed that flight paths are collision-free. For the sake of simplicity, no atmospheric condition, such as wind [26], is taken into consideration, but the inclusion of environmental conditions does not change the overall problem formulation.

There is a camera at the bottom of the aircraft to capture images from the AOIs. The coverage of the camera is studied rather than the detections in images (the measurements). Sensor capabilities (e.g., scan angle, scan direction and coverage radius) are assumed to be constant during the mission time for each aircraft and same for all aircraft. Therefore, the cells in AOIs are of the same size.

Base stations are located out of AOIs (see Fig. 1) and their locations are known a priori. An aircraft has already been assigned to a base station. Each base station has one or more aircraft. In the following, when we refer to an aircraft, the corresponding base station is designated and specified.

A mission time is given and each aircraft should land at the base by the end of the mission plan. An aircraft may take off and land multiple times in the mission horizon.

The mission objective is to maximize information collected via AOI coverage: aircraft should strive to cover as many cells as possible and make full use of their flight time to cover visited or unvisited cells. The persistent monitoring of a particular AOI and the survey of different AOIs are both desired. However, it is always difficult to achieve the above two goals simultaneously when assets are limited. To address this, a revisit requirement to ensure prompt update of surveillance information is used: each cell inside AOIs is to be covered within a given time interval, e.g., within each 8-hour slot.

B. Mission Plan

A flight is one sortie of an aircraft, which consists of a sequence of waypoints (bases and POIs) that starts from a base, visits a group of POIs and turns back to the same base from which the aircraft departs, as shown in Fig. 2. A flight is also referred to as a single-period path (sp) in this paper. For one aircraft, there are multiple flights in the mission plan. The connection of multiple single-period paths with the take-off time for each flight forms a multi-period path (mp). A mission plan consists of the multi-period path for each aircraft. The paths are to be planned and the take-off time schedule is to be determined for each mission plan, in which aircraft survey AOIs cooperatively in space and time.

The visit time point of each POI is recorded along with the planned path, which forms a visiting time sequence. In other words, the mission planner registers aircraft's arrival time at each POI. Once the mission plan is derived, the multiple visits of one POI by all aircraft correspond to a set of visit time, which can be sorted in a chronological order. Then the revisit time interval of this POI can be calculated. Based on the planned paths and the visit time of each POI, the performance of the mission plan can be evaluated, which will be described as follows.

C. Mission Objective Evaluation

Since the cells are of the same size, we use the number of covered cells (visited POIs) to evaluate the coverage. The

0018-9251 (c) 2018 IEEE. Personal use is permitted, but republication/redistribution requires IEEE permission. See http://www.ieee.org/publications_standards/publications/rights/index.html for more information.

This article has been accepted for publication in a future issue of this journal, but has not been fully edited. Content may change prior to final publication. Citation information: DOI 10.1109/TAES.2018.2812538, IEEE Transactions on Aerospace and Electronic Systems

mission objective is evaluated by two metrics: 1) the number of non-repeatedly visited POIs in a sliding-window fashion (referred to as the *revisit-unrepeated* metric), and 2) the total number of visited POIs in the mission plan (referred to as the *revisit-total* metric). These two metrics are proposed based on the following assumptions:

1) Even though the mission lasts for a very long time, the user wants to know the overall situation in each AOI as soon as possible. Therefore, covering different POIs/AOIs is more important than continuously covering a particular POI/AOI.

2) The probability of new information gathered from a particular POI increases with time. Revisiting a POI contributes to the information collected. However, revisiting a POI immediately contributes little to the collected information [11]. If an aircraft still has the capacity (e.g., fuel) to cover cells after all POIs are visited, it should continue covering to achieve a greater number of revisited POIs.

Given a mission plan, the *revisit-unrepeated* metric is evaluated in a sliding window fashion [5]. The initial time of the sliding window is the start time of the mission. The size and the step length of the sliding window are fixed, where the length is much smaller than the mission time. The window is moved over the time horizon to evaluate the *revisit-unrepeated* metric. In each time window, revisit to a POI does not increase the *revisit-unrepeated* metric value. Therefore, an aircraft should visit as many different POIs as possible and avoid revisiting within the window if maximizing the *revisit-unrepeated* metric is used as the only objective. However, if an aircraft has enough fuel after all AOIs are covered, it will return to the base instead of fully using its capacity to cover when maximizing the *revisit-unrepeated* metric is its only objective.

Since the *revisit-unrepeated* metric cannot direct aircraft to revisit POIs and make full use of the surveillance capabilities of aircraft, the *revisit-total* metric is developed as a complement to the *revisit-unrepeated* metric. All visited POIs in the mission plan are counted in the *revisit-total* metric. However, if maximizing the *revisit-total* metric is the only objective, aircraft will keep surveying the nearest AOI without the need to leave it [11]. The result is that no information is gathered from other AOIs in the mission plan. Thus, both the *revisit-unrepeated* metric and the *revisit-total* metric are needed.

III. Problem Formulation

A. Notations and Definitions

The proposed problem is defined on a complete directed graph comprising a set V of vertices or waypoints (that represents the physical locations of POIs and bases) together with a set of edges connecting each pair of vertices. The set V is further partitioned into two subsets: $V = S \cup B$, where S is the set of POIs to be visited and B is the set of base stations. The set of aircraft is denoted as A and the set of AOIs as E. A list of symbols and notations used in this paper is given in Tabel I.

The decision variables are the take-off time and the path selection for each flight. Let t_{b1aw} denote the take-off time of aircraft a in its w-th flight from base b_a, where $w \in W_a$ and $0 \leq t_{b1aw} < T_{\mathrm{m}}$ (the mission start time is used as the zero time reference). Since once the aircraft is specified, the corresponding base of this aircraft is also identified, the subscript of b_a is omitted in t_{b1aw}. In the following, we will omit the subscript of b_a when a and b_a are both in the notation. Let $x_{i\kappa j\mu aw}$ denote the path selection binary decision variable:

TABLE I: Symbols and Notations

Symbol	Description
b_a	base for aircraft a (known a priori), $a \in A$, $b_a \in B$
S_e	set of POIs inside AOI e, $e \in E$, $S_e \subseteq S$
v_a	speed of aircraft a
d_{ij}	travel distance (by the shortest path) from vertex i to vertex j, $\{i,j\} \in V$
C_{ija}	travel time from vertex i to vertex j by aircraft a. $C_{ija} = d_{ij}/v_a$
T_a^{f}	the maximum flight time of aircraft a
T_a^{dmin}	the minimum downtime of aircraft a between two successive flights
T_a^{dmax}	the maximum downtime of aircraft a between two successive flights
T_{h}	a time slot aircraft landing at base
T_{m}	mission time
T_{r}	required revisit time interval: each POI should be revisited within T_{r}
T_{c}	sliding window size
δ	step length of the sliding window
W_a	set of flights of aircraft a
N_a^W	total number of flights of aircraft a (the cardinality of W_a, $\lvert W_a \rvert = N_a^W$)
F_{iaw}	set of visit time indices of vertex i in the w-th flight of aircraft a, $i \in V$, $a \in A$, $w \in W_a$
K_i	set of visit time indices of POI i in the mission plan by all aircraft, $i \in S$

$$x_{i\kappa j\mu aw} = \begin{cases} 1 & \text{if the } \kappa\text{-th visit to vertex } i \text{ is followed by the } \mu\text{-th visit to vertex } j \text{ in the } w\text{-th flight of aircraft } a,\ i \neq j \\ 0 & \text{otherwise} \end{cases} \tag{1}$$

When the path selection decision variables $x_{i\kappa j\mu aw}$ are determined, a path is formed [19, 28]. In the proposed problem, a single-period path for the w-th flight of aircraft a at base b_a is defined as:

$$\begin{aligned} \mathrm{sp}_{aw} = \{b_a, \overbrace{k, \cdots, l}^{\text{POIs}}, b_a \mid\ & x_{i\kappa j\mu aw}, \\ & \forall \kappa \in F_{iaw},\ \mu \in F_{jaw},\ \{i,j\} \in V\}, \end{aligned} \tag{2}$$

where the starting vertex and the ending vertex are the same

0018-9251 (c) 2018 IEEE. Personal use is permitted, but republication/redistribution requires IEEE permission. See http://www.ieee.org/publications_standards/publications/rights/index.html for more information.

This article has been accepted for publication in a future issue of this journal, but has not been fully edited. Content may change prior to final publication. Citation information: DOI 10.1109/TAES.2018.2812538, IEEE Transactions on Aerospace and Electronic Systems

base station b_a, κ and μ are the visit time indices of POIs in a single flight.

In the proposed problem, one POI is allowed to be visited more than once in a single-period path. Moreover, an aircraft can fly from POI i to POI j more than once in a single flight to revisit POIs. If $x_{ij}=1$ is used to denote a visit to vertex i is followed by a visit to vertex j [24, 34], the notation x_{ij} cannot refer to the multiple path selections from vertex i to vertex j caused by revisiting in a single-period path. Hence, the classical notations in VRPs [24] will lead to ambiguity in the formulation of our problem. To address this, $\{\gamma,\eta,\kappa,\mu\}$ are used to denote the visit time indices of POIs. The visit of a POI becomes unique in a single-period path, when the visit time index is associated with the POI.

When the planned single-period path, take-off time, speed of aircraft and the locations of vertices are given, the visit time of POIs in this path and the landing time at the base can be computed. The κ-th visit time of POI i by aircraft a's w-th flight is denoted as $t_{i\kappa aw}$, where $\kappa\in F_{iaw}$. When $i=b_a$ and $\kappa=1$, the notation $t_{i\kappa aw}$ becomes t_{b1aw}, which is the take-off time. The landing time of aircraft a at base b_a is defined as t_{b2aw}, which also conforms to the format of notation $t_{i\kappa aw}$ (when $i=b_a$, $\kappa=2$). The formulation of $t_{i\kappa aw}$ will be provided in Section III-B.

The multi-period path for aircraft a is defined as $\mathrm{mp}_a=\{\mathrm{sp}_{aw},\ t_{b1aw},\ \forall w\in W_a\}$. The total number of flights N_a^W of aircraft a is determined when each flight is planned and connected, and is not known a priori. The take-off time schedule for every aircraft in the mission plan is denoted as $T_0=\{t_{b1aw},\ \forall a\in A,\ b_a\in B,\ w\in W_a\}$. The mission plan is $P=\{\mathrm{mp}_a,\ \forall a\in A\}$. Therefore, a mission plan is formed by determining the path selection and take-off time decision variables for each flight. These decision variables enable the spatio-temporal cooperation of aircraft to cover AOIs and jointly affect the performance of the mission.

B. Problem Formulation

We first provide the calculation for the visit time and the revisit time interval of a POI, and then derive the formulations for the objective functions. Finally, the constraints are discussed.

For the w-th flight of aircraft a, suppose the generated path is sp_{aw} and the corresponding take-off time is t_{b1aw}. Consider this path only and ignore the cooperation across multiple aircraft. The time point that POI k is visited by aircraft a for the γ-th time in this path is:

$$\begin{aligned}t_{k\gamma aw}=t_{b1aw}&+\sum_{i\in V}\sum_{j\in S}\sum_{\kappa\in F_{iaw}}\sum_{\mu\in F_{jaw}}C_{ija}x_{i\kappa j\mu aw}\\&+\sum_{l\in V}\sum_{\eta\in F_{law}}C_{lka}x_{l\eta k\gamma aw},\end{aligned}\tag{3a}$$

$$\begin{aligned}&\{u_{i\kappa aw},\ u_{j\mu aw},\ u_{l\eta aw}\}<u_{k\gamma aw},\\&\forall a\in A,\ b_a\in B,\ w\in W_a,\ \{i,l\}\in V,\ \{j,k\}\in S,\\&\kappa\in F_{iaw},\ \mu\in F_{jaw},\ \eta\in F_{law},\ \gamma\in F_{kaw},\end{aligned}\tag{3b}$$

where the additional real variables $\{u_{i\kappa aw},\ u_{j\mu aw},\ u_{l\eta aw},\ u_{k\gamma aw}\}$ in (3b) are used to order all vertices [27], which follow the Miller-Tucker-Zemlin subtour elimination constraints (MTZ-SECs) [22]. The formulations of MTZ-SECs using $\{u_{i\kappa aw},\ u_{j\mu aw},\ u_{l\eta aw},\ u_{k\gamma aw}\}$ will be provided later in this section. The total number of visited POIs (with repeat) in sp_{aw} can be expressed as

$$n_{aw}=\sum_{i\in V}\sum_{j\in S}\sum_{\kappa\in F_{iaw}}\sum_{\mu\in F_{jaw}}x_{i\kappa j\mu aw}.\tag{4}$$

The variable $u_{i\kappa aw}$ satisfies

$$u_{i1aw}=1,\ i=b_a,\tag{5a}$$

$$2\le u_{i\kappa aw}\le n_{aw}+1,\ i\in S,\ \kappa\in F_{iaw},\tag{5b}$$

and the variable $u_{i\kappa aw}$ denotes the position of vertex i in path sp_{aw}, while the visit time index of vertex i is κ [27].

The visit time point of each POI in a mission plan can be calculated by (3) when flights for all aircraft are planned. The visited POIs in the mission plan can be sorted by their visit time in chronological order. For POI i, the chronological set of visit times by all aircraft in the mission plan can be formed, which is denoted as K_i.

Let $U_{i\varepsilon P}$ denote the position of POI i in mission plan P, where the visit time index of POI i is ε ($\varepsilon\in K_i$). Let $t(U_{i\varepsilon P})$ denote the time point at position $U_{i\varepsilon P}$, which can be obtained after sorting $t_{i\kappa aw}$ for all $a\in A$, $b_a\in B$, $w\in W_a$, $\kappa\in F_{iaw}$. The revisit time interval between the $(\varepsilon-1)$-th visit and the ε-th visit of POI i in the mission plan is expressed as:

$$\mathrm{rvt}(i,\varepsilon)=t(U_{i\varepsilon P})-t(U_{i(\varepsilon-1)P}),\quad \varepsilon>1,\ \varepsilon\in K_i,\tag{6}$$

where $\mathrm{rvt}(\cdot)$ stands for the revisit time interval. The first visit time of POI i is denoted as $\mathrm{rvt}(i,1)=t(U_{i1P})$, $\forall i\in S$. It is required that the first visit of each POI happen within T_r after the mission starts.

In the following, we provide the evaluation of the *revisit-unrepeated* metric in the sliding windows.

A sliding window with size T_c and step length δ moves over the mission time horizon. The total number of windows is $N_\tau=(T_\mathrm{m}-T_\mathrm{c})/\delta+1$. The value of δ should guarantee that the end time of the last evaluation window is the mission time. Usually, δ is less than T_c so that all visited POIs in the mission plan are included in the sliding windows. The τ-th evaluation window starts from $(\tau-1)\delta$ and ends at $T_\mathrm{c}+(\tau-1)\delta$, where $\tau=1,2,\cdots,N_\tau$.

The visited POIs in mission P, whose visit time drops into the τ-th evaluation window, is the set of POIs under test:

$$\begin{aligned}Q(\tau)=\{&\forall i\in S\mid(\tau-1)\delta\le t(U_{i\varepsilon P})\le T_\mathrm{c}+(\tau-1)\delta,\\&\forall\varepsilon\in K_i\}.\end{aligned}\tag{7}$$

For POIs in $Q(\tau)$, define a binary variable $y(i,\tau)$

$$y(i,\tau)=\begin{cases}1 & \text{if POI } i\in Q(\tau)\\ 0 & \text{otherwise}\end{cases}\tag{8}$$

The condition for $y(i,\tau)=1$ means that POI i is visited at least once in the τ-th window. Therefore, repeated visit to a POI in the evaluation window does not increase the value of

0018-9251 (c) 2018 IEEE. Personal use is permitted, but republication/redistribution requires IEEE permission. See http://www.ieee.org/publications_standards/publications/rights/index.html for more information.

This article has been accepted for publication in a future issue of this journal, but has not been fully edited. Content may change prior to final publication. Citation information: DOI 10.1109/TAES.2018.2812538, IEEE Transactions on Aerospace and Electronic Systems

$y(\cdot)$.

The *revisit-unrepeated* metric in the τ-th sliding window is defined as the sum of $y(i,\tau)$ with respect to (w.r.t.) all POIs: $\sum_{i\in S} y(i,\tau)$. To evaluate the *revisit-unrepeated* metric in the mission plan, we present a maximin criteria [19] that maximizes the minimum *revisit-unrepeated* metric in all evaluation windows. The minimum *revisit-unrepeated* metric is defined as:

$$f_1 = \min(\sum_{i\in S} y(i,\tau),\ \forall\tau = 1,2,\cdots,N_\tau). \tag{9}$$

The first objective is expressed as:

$$\max_{P}\ f_1. \tag{10}$$

There are other ways to evaluate the *revisit-unrepeated* metric, e.g., $\sum_{\tau=1}^{N_\tau}\sum_{i\in S} y(i,\tau)$. Since there are overlapping time slots between two evaluation windows, adding up $\sum_{i\in S} y(i,\tau)$ in all windows is not used in our method but the maximin criteria as shown in (9) and (10) are used.

The evaluation of the *revisit-total* metric is the sum of all visited POIs in the mission plan, which is expressed as:

$$\begin{aligned} f_2 =& \sum_{a\in A}\sum_{w\in W_a}\sum_{i\in V}\sum_{j\in S}\sum_{\kappa\in F_{iaw}}\sum_{\mu\in F_{jaw}} x_{i\kappa j\mu aw} \\ =& \sum_{a\in A}\sum_{w\in W_a} n_{aw}. \end{aligned} \tag{11}$$

The second objective, maximizing the total number of visited POIs, is expressed as:

$$\max_{P}\ f_2. \tag{12}$$

Note that the decision variables in (10) and (12) are the path selection and the take-off time for each flight. Here, mission plan P is placed in (10) and (12) as the argument for simplicity.

Formulations of constraints are listed as follows:

$$\begin{aligned} &\sum_{i\in S}\sum_{\kappa\in F_{iaw}} x_{k1i\kappa aw} = \sum_{j\in S}\sum_{\mu\in F_{jaw}} x_{j\mu k2aw} = 1, \\ &\forall a\in A,\ w\in W_a,\ k = b_a \end{aligned} \tag{13}$$

$$\begin{aligned} &\sum_{i\in S}\sum_{\kappa\in F_{iaw}} x_{k1i\kappa aw} = 0, \\ &\forall a\in A,\ w\in W_a,\ k\in B\setminus\{b_a\} \end{aligned} \tag{14}$$

$$\begin{aligned} &\sum_{i\in V}\sum_{\kappa\in F_{iaw}} x_{i\kappa k\gamma aw} = \sum_{j\in V}\sum_{\mu\in F_{jaw}} x_{k\gamma j\mu aw} \le 1, \\ &\forall a\in A,\ w\in W_a,\ k\in S,\ \gamma\in F_{kaw} \end{aligned} \tag{15}$$

$$\begin{aligned} &\sum_{i\in V}\sum_{j\in V}\sum_{\kappa\in F_{iaw}}\sum_{\mu\in F_{jaw}} C_{ija}x_{i\kappa j\mu aw} \le T_a^{\mathrm{f}}, \\ &\forall a\in A,\ w\in W_a \end{aligned} \tag{16}$$

$$\begin{aligned} &t_{b1a(w+1)} \ge t_{b1aw} + \\ &\sum_{i\in V}\sum_{j\in V}\sum_{\kappa\in F_{iaw}}\sum_{\mu\in F_{jaw}} C_{ija}x_{i\kappa j\mu aw} + T_a^{\mathrm{dmin}}, \\ &\forall a\in A,\ b_a\in B,\ w = 1,\cdots,N_a^W - 1 \end{aligned} \tag{17}$$

$$\begin{aligned} &t_{b1a(w+1)} \le t_{b1aw} + \\ &\sum_{i\in V}\sum_{j\in V}\sum_{\kappa\in F_{iaw}}\sum_{\mu\in F_{jaw}} C_{ija}x_{i\kappa j\mu aw} + T_a^{\mathrm{dmax}}, \\ &\forall a\in A,\ b_a\in B,\ w = 1,\cdots,N_a^W - 1, \end{aligned} \tag{18}$$

$$\begin{aligned} &t_{b1aw} + \sum_{i\in V}\sum_{j\in V}\sum_{\kappa\in F_{iaw}}\sum_{\mu\in F_{jaw}} C_{ija}x_{i\kappa j\mu aw} \le T_{\mathrm{m}}, \\ &\forall a\in A,\ b_a\in B,\ w = N_a^W \end{aligned} \tag{19}$$

$$\mathrm{rvt}(i,\varepsilon) \le T_{\mathrm{r}}, \quad \forall i\in S,\ \varepsilon\in K_i \tag{20}$$

$$\begin{aligned} &2 \le u_{k\gamma aw} \le n_{aw} + 1, \\ &\forall a\in A,\ w\in W_a,\ k\in S,\ \gamma\in F_{kaw} \end{aligned} \tag{21}$$

$$\begin{aligned} &u_{l\eta aw} - u_{k\gamma aw} + 1 \le n_{aw}\left(1 - x_{l\eta k\gamma aw}\right), \\ &\forall a\in A,\ w\in W_a,\ \{l,k\}\in S,\ \eta\in F_{law},\ \gamma\in F_{kaw} \end{aligned} \tag{22}$$

$$\begin{aligned} &x_{i\kappa j\mu aw}\in\{0,1\},\ t_{b1aw}\ge 0, \qquad \forall a\in A,\ b_a\in B, \\ &w\in W_a,\ \{i,j\}\in V,\ \kappa\in F_{iaw},\ \mu\in F_{jaw} \end{aligned} \tag{23}$$

Constraint (13) guarantees that an aircraft starts from its base station and ends at the same base station in each flight. Constraints (13) and (14) guarantee that an aircraft only take off from the base specified to this aircraft, where the backslash symbol $\setminus$ in (14) denotes a set difference.

Constraint (15) guarantees the connectivity of POIs in each flight. When the γ-th visit to POI k in the w-th flight of aircraft a is given, $\sum_{i\in V}\sum_{\kappa\in F_{iaw}} x_{i\kappa k\gamma aw}$ equals 0 or 1.

When a path is planned, the continuity of time sequence is guaranteed:

$$\begin{aligned} &t_{i\kappa aw} + C_{ija} - t_{j\mu aw} \le M\left(1 - x_{i\kappa j\mu aw}\right), \\ &\forall a\in A,\ w\in W_a,\ \{i,j\}\in V,\ \kappa\in F_{iaw},\ \mu\in F_{jaw}, \end{aligned} \tag{24}$$

where M is a very large positive constant ($M \gg T_{\mathrm{m}}$). If there exists a path selection from the κ-th visit of vertex i to the μ-th visit of vertex j in aircraft a's w-th flight, $x_{i\kappa j\mu aw} = 1$, and $t_{i\kappa aw} + C_{ija} - t_{j\mu aw} = 0$.

Constraint (16) ensures that the travel time of each flight is no more than the maximum flight time.

Constraints (17) and (18) ensure that the downtime between two successive flights is no less than the minimum downtime and no greater than the maximum downtime, respectively. The wait time in addition to the minimum downtime before the $(w+1)$-th flight of aircraft a is denoted as

$$\begin{aligned} h_{aw} =& t_{b1a(w+1)} - t_{b1aw} - \\ &\sum_{i\in V}\sum_{j\in V}\sum_{\kappa\in F_{iaw}}\sum_{\mu\in F_{jaw}} C_{ija}x_{i\kappa j\mu aw} - T_a^{\mathrm{dmin}}, \end{aligned} \tag{25}$$

0018-9251 (c) 2018 IEEE. Personal use is permitted, but republication/redistribution requires IEEE permission. See http://www.ieee.org/publications_standards/publications/rights/index.html for more information.

This article has been accepted for publication in a future issue of this journal, but has not been fully edited. Content may change prior to final publication. Citation information: DOI 10.1109/TAES.2018.2812538, IEEE Transactions on Aerospace and Electronic Systems

where $h_{aw} \leq T_a^{\text{dmax}} - T_a^{\text{dmin}}$. It will be shown in Section IV that the take-off time schedule is generated by determining the take-off time of the first flight t_{b1a1} and the following wait time h_{aw} $\left(w = 1, \cdots, N_a^W - 1\right)$.

Constraint (19) guarantees that the time point of aircraft returning to base for the last flight is not greater than the mission time.

Constraint (20) guarantees that each POI is visited for the first time within T_{r} after the mission starts (for the case $\varepsilon = 1$), and that each POI is revisited within T_{r} for the following visits (for the cases $\varepsilon > 1$). The revisit time interval $\text{rvt}(\cdot)$ is calculated as (6).

Constraints (21) and (22) are used to prevent subtours in each single-period path, which are derived from MTZ-SECs [1, 22]. The total number of visited POIs in the w-th flight of aircraft a is n_{aw} as in (4), where the repetition of POIs is considered.

IV. Solution Technique

The proposed mission planning problem is more complex than the existing VRPs and OPs because of the revisiting in single-period paths and the spatio-temporal cooperation of aircraft in multi-period paths. Furthermore, only small instances of the VRP or OP can be solved exactly [6, 30]. It is clear that one cannot solve this path planning and scheduling with the above formulation. We have therefore opted for the development of an MOEA. The choice is motivated by 1) the success of EA in VRP and its variants [10, 35], and 2) the ability of MOEA to find multiple Pareto-optimal solutions or converge near the true Pareto-optimal set in one single simulation run [8].

The flowchart of the path planning and scheduling algorithm is illustrated in Fig. 3. The algorithm consists of four parts: pre-processing, multi-objective evolution, decision making, and waypoint transformation. This paper mainly describes methods in the pre-processing and the multi-objective evolution.

At the very beginning, parameters are initialized, AOIs are divided into cells, and POIs are generated. Single-period paths are generated by solving a series of OPs, in which revisit to POIs and take-off time schedule are not considered. For one aircraft, these single-period paths are connected to form the multi-period path, where the take-off time of each flight is randomly selected under constraints.

A set of mission plans is generated as the initial population in the EA, where the paths for all aircraft are evaluated as shown in (9) to (12). The revisit constraint (20) is transformed into an objective function in the EA, which will be described later in this section.

During the evolution of individuals, rescheduling of take-off time and revisit to POIs are enabled by the mutation operator; exchanging single-period paths between mission plans is conducted by the crossover operator. These genetic operators differ from standard mutation and crossover [15] and are especially designed for the proposed problem. Objective functions are evaluated and sorted following the non-dominated sorting genetic algorithm II (NSGA-II) procedure [8].

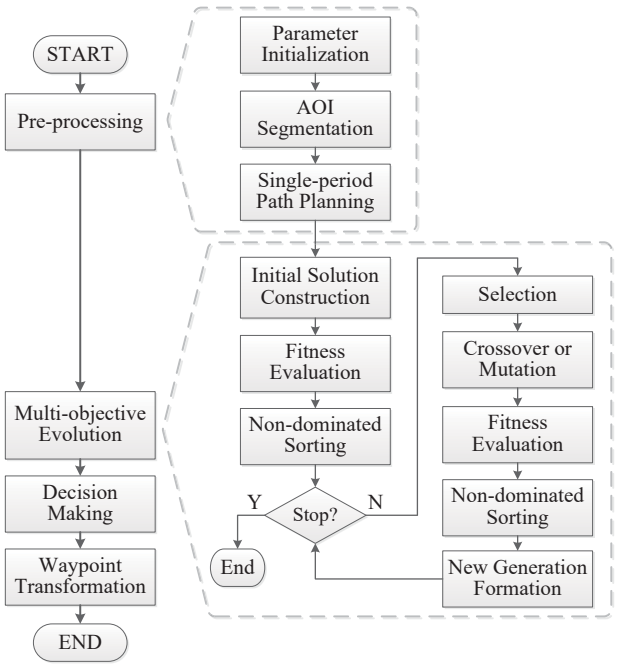

Fig. 3: Flowchart of the coverage path planning and scheduling algorithm.

The best mission plan is selected by a weighted-sum model in decision making from the MOO solution set. The mission plan generated by the steps described above is a sequence of vertices, which correspond to ground locations/waypoints. Finally, paths are transformed into aerial waypoints for each aircraft based on the aircraft motion model (e.g., Dubins airplane) [13, 20] and sensor parameters [18]. However, waypoint transformation is not the focus of this paper.

A. Mission Plan Structure

The mission plan structure is also the genetic representation of an individual (chromosome), which is shown in Fig. 4. The mission plan for one aircraft is made up of multiple single-period paths connected by elements representing the state of aircraft landing at the base. The wait time before the first flight and the wait time in addition to the minimum downtime are discretized into time slots with a fixed length of T_{h}. The genetic representation of the minimum downtime is D and that of the discrete time slot is H. The genetic representation of POI i is s_i and that of base for aircraft a is b_a.

As shown in Fig. 4, the number of H affects the take-off time: aircraft can take off immediately after the minimum downtime or stay at the base for several time slots. When the time left is not enough for the aircraft to visit the nearest POI at the end of the mission, this remaining time is denoted as several time slots as well. This is because taking off, in this case, will not increase the objective values. The determination of the number of time slots before each flight will be described later in this section.

Given the mission plan structure, a time table for each aircraft, which consists of the take-off time of each flight, the visit time of POIs, the landing time of each flight, and

0018-9251 (c) 2018 IEEE. Personal use is permitted, but republication/redistribution requires IEEE permission. See http://www.ieee.org/publications_standards/publications/rights/index.html for more information.

This article has been accepted for publication in a future issue of this journal, but has not been fully edited. Content may change prior to final publication. Citation information: DOI 10.1109/TAES.2018.2812538, IEEE Transactions on Aerospace and Electronic Systems

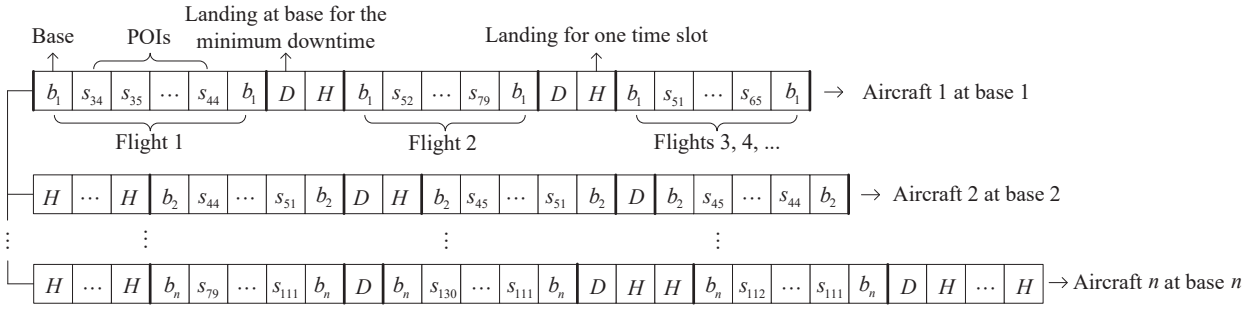

Fig. 4: Mission plan structure.

minimum downtime and the wait time slots, can be computed. Elements in the mission plan and time points in the time tables have one-to-one correspondence. The mission plan structure, along with the time tables, effectively handles the path selection and the take-off time decision at the same time. It also manipulates the variable-length chromosome, which makes the EA easy to operate [14, 29].

B. Single-period Path Planning

Single-period paths are the construction blocks in the mission plan. By connecting the single-period paths and determining the take-off time for each flight, the initial population to EA can be generated, which has the potential to achieve the mission goal, as described in (9) to (12). Hence, single-period path planning is preliminary to the construction of initial population of EA.

The path planning for each aircraft is formulated as a series of OPs. In OP, each POI is associated with a score, the goal is to determine a path with a maximum sum of the collected scores in limited length [34]. Each POI is visited at most once in these paths.

Let T_a^{lmt} denote a set of time limits for aircraft a: $T_a^{\text{lmt}} = \{t_a^{\text{lmt}}(\phi),\ \phi = 1, 2, \cdots\}$, which may range from a small value (e.g., the time needed to fully cover the nearest AOI by aircraft a) to the maximum flight time T_a^{f} with a fixed step size. Within the given time interval $t_a^{\text{lmt}}(\phi)$, paths are designed to maximize the collected scores associated with POIs. Initially, POIs are assigned with the same scores to generate the first path by solving the OP. When the path is generated, unvisited POIs within this aircraft's reach (limited by $t_a^{\text{lmt}}(\phi)$) are assigned with higher scores than already visited POIs; an OP is solved again to visit POIs with the updated scores. The score of a POI depends on whether this POI is visited or not in the already planned paths. This process continues until all POIs within the aircraft's reach are visited. Then, the time limit increases and paths are planned by the above approach once again.

By assigning higher scores to unvisited POIs, single-period paths are generated to cover unvisited POIs within the aircraft's reach. Paths with different POIs enrich the diversity of single-period paths. Unvisited POIs in a flight can be explored either by the same aircraft's subsequent flights or by other aircraft. Because of the different time limits, paths of different time length are included in the mission plan. By connecting these paths of different lengths, multi-period paths with different flight number N_a^W can be generated, which enrich the diversity of multi-period paths. When the time limit $t_a^{\text{lmt}}(\phi)$ is less than the maximum flight time, it is possible to use the remaining time $(T_a^{\text{f}} - t_a^{\text{lmt}}(\phi))$ to revisit POIs by the mutation operator. Therefore, solving the proposed series of OPs ensures the diversity of the mission plan.

The path planning decision variable in OP is defined as:

$$x_{ij} = \begin{cases} 1 & \text{if a visit to vertex } i \text{ is followed by a visit to vertex } j \\ 0 & \text{otherwise} \end{cases} \tag{26}$$

Given the scores for each POI, one OP for aircraft a at base b_a is formulated as:

$$\max_{x_{ij}} \quad \sum_{i\in S}\sum_{j\in V} \text{sc}(i)x_{ij} \tag{27}$$

$$\text{s.t.} \quad \sum_{j\in S} x_{kj} = \sum_{i\in S} x_{ik} = 1, \quad k = b_a \tag{28}$$

$$\sum_{i\in V} x_{ik} = \sum_{j\in V} x_{kj} \le 1, \quad \forall k \in S \tag{29}$$

$$\sum_{i\in V}\sum_{j\in V} C_{ija}x_{ij} \le t_a^{\text{lmt}}(\phi),\ \forall t_a^{\text{lmt}}(\phi) \in T_a^{\text{lmt}} \tag{30}$$

$$2 \le u_k \le \sum_{i\in V}\sum_{j\in V} x_{ij}, \quad \forall k \in S \tag{31}$$

$$u_l - u_k + 1 \le \sum_{i\in V}\sum_{j\in S} x_{ij}\left(1 - x_{lk}\right), \quad \forall\{l,k\} \in S \tag{32}$$

$$x_{ij} \in \{0,1\}, \quad \forall\{i,j\} \in V \tag{33}$$

where $\text{sc}(i)$ is the score assigned to POI i, u_i is the position of vertex i in the path [27, 34]. The purpose of objective function (27) is to maximize the total collected score. Constraint (28) guarantees that the paths start and end at the same base. Constraint (29) ensures the connectivity of the POIs in the path. Constraint (30) ensures the limited time budget. Constraints (31) and (32) are necessary to prevent subtours [34]. The constraints (28), (29), (30), (31) and (32) correspond to (13), (15), (16), (21) and (22), respectively. A five-step heuristic is used to solve the OP [3].

For the series of OPs, the solution is described in Algorithm 1, where the updating of scores and the traversing of time limits are shown. In Algorithm 1, C_{bia} represents the

0018-9251 (c) 2018 IEEE. Personal use is permitted, but republication/redistribution requires IEEE permission. See http://www.ieee.org/publications_standards/publications/rights/index.html for more information.

This article has been accepted for publication in a future issue of this journal, but has not been fully edited. Content may change prior to final publication. Citation information: DOI 10.1109/TAES.2018.2812538, IEEE Transactions on Aerospace and Electronic Systems

travel time from base b_a to POI i by aircraft a; S_{ab} is a set of POIs within the reach of aircraft a taking off from base b_a; $S(\text{unvisit})$ is a set of unvisited POIs in S_{ab}; $\text{sp}_{\text{cnt}}^{\phi}$ denotes the single-period path generated in the cnt-th iteration of the ϕ-th time limit; $\emptyset$ denotes the empty set. Note that different values of ρ ($\rho > 1$) lead to different paths: the greater the ρ, the more unvisited POIs will be included in the path. All planned paths are stored to ensure the population diversity in the EA.

Algorithm 1 Single-period path planning

Input:
Aircraft a. Base station b_a. Set of POIs S.
Fixed score c. Factor ρ. Set of time limits T_a^{lmt}.
Output:
Single-period paths $\text{sp}_{\text{cnt}}^{\phi}$,
$\phi = 1, 2, \cdots, |T_a^{\text{lmt}}|$, $\text{cnt} = 1, 2, \cdots$.

for $t_a^{\text{lmt}}(\phi) \in T_a^{\text{lmt}}$ **do**
  $S_{ab} = \left\{ i | 2C_{bia} \le t_a^{\text{lmt}}(\phi),\ i \in S \right\}$
  $S(\text{unvisit}) = S_{ab}$
  Counter $\text{cnt} = 1$
  Score $\text{sc}(i) = c$, $\forall i \in S_{ab}$
  while $S(\text{unvisit}) \neq \emptyset$ **do**
    Solve OP: (27)–(33), generate and save $\text{sp}_{\text{cnt}}^{\phi}$
    Update $S(\text{unvisit}) = \left\{ i | i \in S_{ab}\ \&\ i \notin \bigcup_{\text{cnt}} \text{sp}_{\text{cnt}}^{\phi} \right\}$
    Update $\text{sc}(i) = \rho^{\text{cnt}} c$, $\forall i \in S(\text{unvisit})$
    $\text{cnt} = \text{cnt} + 1$
  end while
end for

Note that no-fly zones [9, 11] outside AOIs are not considered in the mission scenario, but no-fly zones can be handled in our solution technique. A discussion on no-fly zones in single-period path planning is provided in the Appendix.

C. Initial Population Construction

Instead of planning the path by randomly picking up POIs and randomly setting the take-off time, well-designed single-period paths are used as the construction blocks for the initial population, and the take-off time for each flight is randomly configured with constraints. For one aircraft, its single-period paths are connected as shown in Fig. 4. The path for each flight is randomly selected from the results of single-period path planning except the path for the last flight: the selection of a single-period path for the last flight is constrained by (19). The number of additional wait time slots is determined such that constraints (17) and (18) are satisfied.

As mentioned in Section IV-A, the number of wait time slots affects the take-off time. There are many ways to determine the number of wait time slots for the initial population. For example, a random number l_a can be generated from a discrete uniform distribution $\mathcal{U}\{0, (T_a^{\text{dmax}} - T_a^{\text{dmin}})/T_{\text{h}}\}$, where $t_{b1aw} = l_a T_{\text{h}}$ is the wait time. Another way is to generate a random number l_a from the rounding result of a truncated normal distribution with zero mean and $(T_a^{\text{dmax}} - T_a^{\text{dmin}})/(mT_{\text{h}})$ standard deviation conditioned on $0 \le l_a \le (T_a^{\text{dmax}} - T_a^{\text{dmin}})/T_{\text{h}}$, where m is a positive constant.

The number of wait time slots l_a is scheduled in the initial population construction and rescheduled in the mutation operator. During our simulations, it was observed that mission plans with less additional wait time achieve better objective values. Therefore, generating l_a from the truncated normal distribution is used in our approach, because the value of m can be tuned so that more mission plans with small wait time can be generated in the population.

Because of the single-period path planning and initial population construction, the initial mission plans satisfy constraints (13) to (19), (21) and (22). Individuals in the initial population do not necessarily satisfy the revisit constraint (20). The handling of (20) is described as follows.

D. Infeasibility Handling

In the EA, the feasibility w.r.t. constraints (15) to (19), (21) and (22) is checked in the genetic operators and infeasible paths or mission plans are discarded. The feasibility w.r.t. constraints (13) and (14) is guaranteed in single-period path planning and will not change by the genetic operators. The revisit constraint (20) is transformed into an objective function in the EA for the following reasons:

1) It is possible that the given assets cannot satisfy the revisit constraint (20) for all POIs, i.e., there is no feasible solution.

2) The scale of the problem (i.e., the number of POIs, the time horizon of the mission plan, etc.) is too large to verify the existence of feasible solutions w.r.t. constraint (20).

If the actual revisit time interval $\text{rvt}(i, \varepsilon)$ (see (6)) is greater than the required revisit time T_{r}, the violated time is $\text{rvt}(i, \varepsilon) - T_{\text{r}}$. The sum of violated revisit time is to be minimized by path planning, take-off time scheduling and aircraft cooperation. Let f_3 denote the negative value of the sum of the violated revisit time:

$$f_3 = -\sum_{i \in S} \sum_{\varepsilon \in K_i} \max\left(\text{rvt}(i, \varepsilon) - T_{\text{r}}, 0\right). \tag{34}$$

The objective is expressed as:

$$\max_{P}\ f_3. \tag{35}$$

Therefore, constraint (20) is transformed into (35) in the EA. The multi-objective function is $\max_P\ (f_1, f_2, f_3)$.

E. Multi-objective Evolution

The MOEA is based on the NSGA-II framework [8]. As shown in Fig. 3, the following evolutionary process is performed in each generation: 1) calculate the fitness functions (9), (11) and (34), and select parents that are a fit for reproduction, 2) perform crossover and mutation operators on the selected parents to produce offspring, and calculate the fitness of offspring, 3) form the intermediate chromosome, which is a concatenation of the current population and the offspring population, and 4) non-domination sort the intermediate chromosome, replacing the unfit individuals with the fit individuals to maintain a constant population size.

Selection: Many selection techniques, such as tournament selection [8] and roulette wheel selection [35], are available. A binary tournament selection is used in this paper. Constrained

0018-9251 (c) 2018 IEEE. Personal use is permitted, but republication/redistribution requires IEEE permission. See http://www.ieee.org/publications_standards/publications/rights/index.html for more information.

This article has been accepted for publication in a future issue of this journal, but has not been fully edited. Content may change prior to final publication. Citation information: DOI 10.1109/TAES.2018.2812538, IEEE Transactions on Aerospace and Electronic Systems

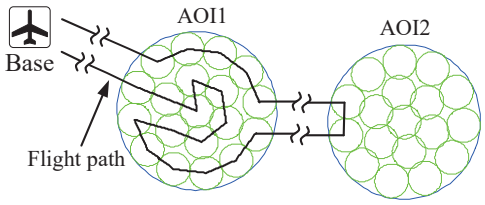

Fig. 5: An example of single-period path. Visited POIs in AOI2 will be removed by *Remove*, and the remaining flight time after *Remove*, especially the travel time between AOI1 and AOI2, is used to revisit POIs in AOI1 when *Insert* is implemented.

NSGA-II (constraint-handling approach) is utilized to rank the solutions [8].

Crossover: Crossover happens with a probability p_{c}. If crossover does not happen, mutation is conducted. From the first flight to the last one, the crossover is performed by exchanging parents' single-period paths (same aircraft, same base station) with a certain probability $p_{\mathrm{c}}^{\mathrm{s}}$ successively, whereas the take-off time of each parent does not change. The time tables of the offspring are updated as the crossover carrying through. If an offspring's actual mission time exceeds T_{m} after a crossover of two single-period paths, this crossover is undone and the single-period paths are reverted to their original (last) positions in the chromosome.

Mutation: The custom mutation operator described in Algorithm 2 is enforced. Three moves are designed for mutation, namely *Remove*, *Insert*, and *Reschedule*.

1) Remove: The goal of *Remove* is, by giving up some visited POIs in a single-period path, to make time for possible revisits of POIs. For instance, the result of *Remove* is that the POIs in AOI2 will not be visited in Fig. 5, and the remaining flight time, especially the travel time between AOI1 and AOI2, will be used to revisit POIs in AOI1 (enabled by *Insert*). Line 7 in Algorithm 2 indicates that POIs in the single-period path of aircraft a's w-th flight (denoted as sp_{aw}), which belong to AOI e but do not constitute the whole POI set in AOI e, are removed. Thus, the spared time can be used to revisit other POIs in the path.

2) Insert: The revisit to POIs is enabled by *Insert*. Some successive POIs within the same AOI in a single-period path are selected as a path segment and inserted into this path, as shown in lines 12 and 13 in Algorithm 2. The length of the path segment can be randomly generated from 1 to $|S_e|$. The locus, where the gene segment is inserted to, should avoid the repeat of the same POI in two successive loci.

3) Reschedule: The take-off time is changed, i.e., the number of T_{h} is generated again (see Section IV-C).

If an offspring violates the maximum flight time constraints or mission time constraints after mutation, the mutation move is undone and the paths are reverted to the original (last) feasible ones, as shown in lines 18 to 20. These three moves can be viewed as heuristic operators embedded in the EA, which take full advantage of the peculiarities of the proposed problem.

Algorithm 2 The custom mutation operator

Input:

A chromosome (i.e., mission plan) P contains

- multi-period paths mp,
- single-period paths sp, and
- take-off time schedule T_0.

Remove probability p_{rm}
Insert probability p_{in}
Reschedule probability p_{rs}

Output:

The mutated chromosome P^* contains

- the mutated multi-period paths mp^*,
- the mutated single-period paths sp^*, and
- the mutated take-off time schedule ${T_0}^*$.

1: **for** $a \in A$ **do**
2: **for** $w \in W_a$ **do**
3: Generate a random number $r \sim \mathcal{U}(0,1)$
4: **if** $r < p_{\mathrm{rm}}$ **then**
5: **for** $e \in E$ **do**
6: **if** $\exists\{\forall i \in \mathrm{sp}_{aw}\} \subsetneq S_e$ **then**
7: *Remove* $\{\forall i \in \mathrm{sp}_{aw}\} \subsetneq S_e$
8: **break**
9: **end if**
10: **end for**
11: **else if** $p_{\mathrm{rm}} \leq r < p_{\mathrm{rm}} + p_{\mathrm{in}}$ **then**
12: Randomly choose an AOI e and a gene segment (GS) within this AOI in a single-period path: GS $\subseteq S_e \subseteq \mathrm{sp}_{aw}$
13: *Insert* GS after a locus to sp_{aw}
14: **else**
15: *Reschedule* t_{b1aw}
16: **end if**
17: Update sp^*_{aw}, mp^*_a and corresponding time tables
18: **if** (travel time of $\mathrm{sp}^*_{aw} > T^{\mathrm{f}}_a$ || mission time of $\mathrm{mp}^*_a > T_{\mathrm{m}}$) **then**
19: Undo this mutation move; revert to the original paths and time tables
20: **end if**
21: **end for**
22: **end for**

F. Decision Making

When the evolution terminates, a set of solutions are generated and the objective values of these solutions are known. Then, we can see if there exist feasible solutions (i.e., $f_3 = 0$) or not w.r.t. constraint (20). A weighted-sum model can be used to integrate the objectives into a single index [33]:

$$\max_{P} \ \boldsymbol{\omega}^T \hat{\boldsymbol{f}}, \tag{36}$$

where $\boldsymbol{\omega} = [\omega_1, \omega_2, \omega_3]^T$, $\omega_1 + \omega_2 + \omega_3 = 1$, $0 \leq \omega_1, \omega_2, \omega_3 \leq 1$, and $\hat{\boldsymbol{f}} = \left[\hat{f}_1, \hat{f}_2, \hat{f}_3\right]^T$. The superscript ^{T} denotes matrix transpose and $\hat{f}_n$ denotes the normalized f_n, where $n = 1, 2, 3$. The selection of weights depends on the user's preferences and priorities. The highest-ranking solution with the greatest

0018-9251 (c) 2018 IEEE. Personal use is permitted, but republication/redistribution requires IEEE permission. See http://www.ieee.org/publications_standards/publications/rights/index.html for more information.

This article has been accepted for publication in a future issue of this journal, but has not been fully edited. Content may change prior to final publication. Citation information: DOI 10.1109/TAES.2018.2812538, IEEE Transactions on Aerospace and Electronic Systems

weighted-sum value will be selected as the mission plan.

If there is no feasible solution w.r.t. constraint (20) in the final solution set, i.e., $f_3 < 0$ for all solutions, the solution with the minimum revisit violation can be selected (by setting $w_3 \gg w_1 + w_2$) if the user emphasizes the revisit constraint. If feasible solutions exist, the mission plan will be selected from these feasible solutions, where $w_1 \geq w_2$, because promptly updating information collected from different POIs is more important than the total number of visited POIs.

The transportation cost (total travel distance) is evaluated as:

$$f_4 = \sum_{a\in A}\sum_{w\in W_a}\sum_{i\in V}\sum_{j\in V}\sum_{\kappa\in F_{iaw}}\sum_{\mu\in F_{jaw}} d_{ij}x_{i\kappa j\mu aw}. \quad (37)$$

If multiple highest-ranking solutions with the same weighted-sum value are found, the one with the minimum transportation cost can be selected as the mission plan.

Note that by adding f_4 to the objective functions $\max_P\ (f_1, f_2, f_3, -f_4)$, minimizing transportation cost joins the optimization as the fourth objective and the proposed algorithm becomes more complex. As the number of objectives increases, the NSGA-II framework may not work efficiently, and the many-objective evolutionary algorithm NSGA-III can be implemented [7, 17]. In this paper, $\max_P\ -f_4$ is not used in the EA.

V. Simulations

A. Mission Scenario

There is no benchmark problem in the literature for the comparison of path planning and scheduling algorithms [11, 23]. Two simulation environments are used in this section for performance evaluation.

In the first simulation scenario, three rectangular regions are simulated as AOIs (see Fig. 6), the sizes of which are 200×160 km^2, 80×80 km^2, and 160×240 km^2. Two aircraft are assigned to two base stations, which are located at $(0, 80)$ km and $(600, 0)$ km, respectively. Aircraft are of the same type. Aircraft fly at a constant speed of 612 km/h with 4-hour maximum flight time. The minimum downtime is 1 hour and the maximum downtime is 1.5 hours. Dots inside the AOIs in the figure are POIs, which are the result of AOI segmentation. The size of each cell is 40×40 km^2. Thus, there are 48 cells in total. The mission lasts for 24 hours. Each POI in the AOIs must be revisited within 8 hours.

The mission scenario of the second simulation is based on a real-world case study, which will be shown later in this section.

B. Termination Condition

Since 1) it is not feasible to compute the global optimal solution of the proposed problem [6, 30], and 2) the NSGA-II framework has the ability to find a diverse set of solutions and converge near the true Pareto-optimal set [8], we specify a termination condition such that the solution at termination is close to the optimal one. The weighted-sum model (36) is implemented at the end of each generation. The best weighted-sum value of objectives is used to determine the termination of the evolution. If the maximum difference of the best (largest) weighted-sum fitness among N_t successive iterations/generations drops below a given threshold, the EA is terminated.

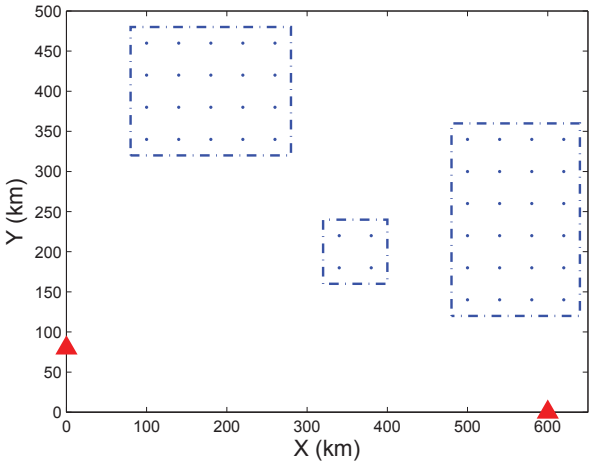

Fig. 6: The first simulation scenario: locations of AOIs, POIs, and base stations.

In the following, different values of crossover and mutation probabilities in two MOOs solution strategies are used to investigate the convergence of the path planning and scheduling problem. The values of crossover probability p_c are 0.3, 0.5, and 0.7; the corresponding mutation probability is $(1 - p_\mathrm{c})$.

The proposed algorithm based on NSGA-II can be viewed as a non-dominated sorting MOO strategy. Except for the proposed algorithm, a weighted-sum MOO strategy, which integrates the objectives into one fitness value in each fitness evaluation as shown in (36), is applied. The weighting vector in these two MOOs is $\boldsymbol{\omega} = [0.25, 0.15, 0.6]^T$.

The difference between the proposed non-dominated sorting MOO and the weighted-sum MOO is where the weighted-sum (36) is implemented. The non-dominated sorting MOO finds multiple solutions in one single simulation run [8] and implements (36) in decision making after the evolution of solutions, whereas the weighted-sum MOO implements (36) in fitness evaluation along with the evolution whenever a new individual is generated.

The crossover probability of each single-period path is $p_\mathrm{c}^s = 0.5$. The probabilities of the moves in the mutation operator are $p_\mathrm{rm} = 0.2$, $p_\mathrm{in} = 0.4$ and $p_\mathrm{rs} = 0.4$. In constructing the chromosome, $T_\mathrm{h} = 1/6$ hours, which means that the wait time after the minimum downtime is an integer multiple of T_h. The truncated normal distribution with $m = 1.5$ is used to determine the number of wait time slots. While evaluating the *revisit-unrepeated* metric, the sliding window size is $T_\mathrm{c} = 4$ hours and the step length $\delta = 1$ hour. Hence, there are $(T_\mathrm{m} - T_\mathrm{c})/\delta + 1 = 21$ evaluation intervals. In this simulation, the population size is set to be 1024. The number of generations in each simulation is 150. The best weighted-sum fitness in each generation is plotted in Fig. 7. The results in the following simulations are based on 100 Monte Carlo

0018-9251 (c) 2018 IEEE. Personal use is permitted, but republication/redistribution requires IEEE permission. See http://www.ieee.org/publications_standards/publications/rights/index.html for more information.

This article has been accepted for publication in a future issue of this journal, but has not been fully edited. Content may change prior to final publication. Citation information: DOI 10.1109/TAES.2018.2812538, IEEE Transactions on Aerospace and Electronic Systems

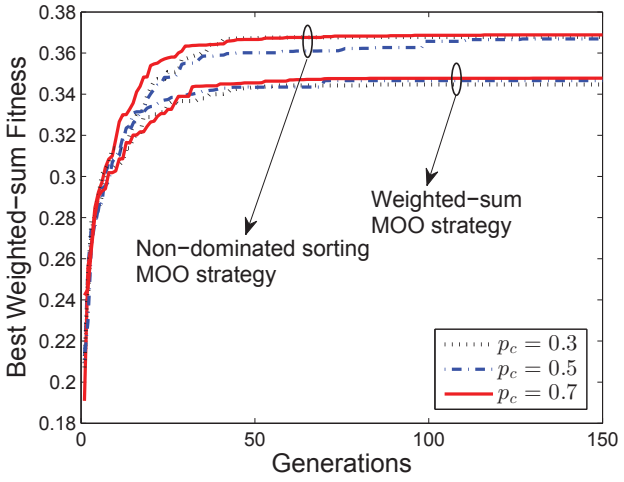

Fig. 7: Best weighted-sum fitness: convergence of the proposed algorithm.

runs.

It can be seen from Fig. 7 that the integrated fitness value reaches a plateau in each simulation with different MOO solution strategies and crossover/mutation probabilities, which shows the convergence of the proposed algorithm. Based on the convergence performance of the proposed algorithm, in the following simulations, the termination condition threshold is set to be 10^{-5}, N_t is set to be 10, and the crossover probability is 0.7.

The weighted-sum model for the objectives can be the other solution strategy for the proposed MOO. Because of avoiding the non-dominated sorting, the weighted-sum MOO strategy requires slightly less computation time in each evolution/generation than the non-dominated sorting MOO strategy. However, the weighted-sum model for MOO is deficient in attaining a diverse set of solutions [21]. The final solution by the weighted-sum MOO is greatly influenced by the selection of the weights in (36). If the user's preferences change, the EA using the weighted-sum MOO strategy is to run again using the new weighting vector.

Our proposed non-dominated sorting MOO strategy enables the attainment of a diverse set of mission plans [8]. The final mission plan can be determined by the weighting vector in decision making, which saves computation time if the user's preferences change or multiple mission plans are needed.

C. Computation Time

The proposed solution procedure is done offline ahead of the mission. Time is mainly spent on two parts: initial population generation and multi-objective evolution. Single-period paths are planned by solving a series of OPs in the initial population generation. The OP is NP-hard (non-deterministic polynomial-time hard) [30] and these OPs are solved by heuristic methods [3], as described in Section IV-B. The number of OPs to solve depends on the topology of mission scenario, the capacity of aircraft and the selection of the time limits T_a^{lmt}. The NSGA-II framework is used to generate a diverse set of mission plans. The computational complexity of NSGA-II is $\mathcal{O}(MN^2)$, where N is the population size and M is the number of objectives [8].

TABLE II: Results for the Problem with Different Objective Functions

Objective function	f_1	f_2
$\max_P\ (f_1, f_2, f_3)$	**41.4**	463.3
$\max_P\ (f_1, f_3)$	41.3	398.8
$\max_P\ (f_2, f_3)$	32.8	**465.7**

This coverage path planning and scheduling problem is solved using MATLAB on a Core™ i7 2.5 GHz CPU with 16 GB RAM. In the above simulation, the population size is 1024, and the number of objectives is 3. The average computation time of initial population generation is 44 seconds. Using the non-dominated sorting MOO strategy, the average computational time of convergence to the final solution by the evolutionary process is 377 seconds. Using the weighted-sum MOO strategy, the average computational time of convergence to the final solution by the evolutionary process is 274 seconds. Note that the proposed algorithm is for offline path planning and scheduling, therefore the computation time is modest.

D. Objectives

In order to illustrate the advantage of using both *revisit-unrepeated* and *revisit-total* as objectives, $\max_P\ (f_1, f_2, f_3)$ is compared with $\max_P\ (f_1, f_3)$ and $\max_P\ (f_2, f_3)$. The values of f_1, f_2 and f_3 are evaluated as (9), (11) and (34) respectively, where the unit of f_3 is hour.

Feasible solutions ($f_3 = 0$) are generated in all cases, because revisit of each POI within 8 hours is not a strong constraint given the mission scenario. It can be seen from Table II that large values of f_1 and f_2 are attained by the proposed objectives $\max_P\ (f_1, f_2, f_3)$. However, when maximization of f_2 is not used as an objective, the value of f_2 is much smaller than that of $\max_P\ (f_1, f_2, f_3)$. Conversely, when maximization of f_1 is not specified as an objective, the largest f_2 is achieved, but f_1 is much smaller than that of $\max_P\ (f_1, f_2, f_3)$. Hence, the multi-objective function used in this paper guarantees prompt update of information from different POIs and a large number of covered cells (visited POIs), which in turn makes a persistent and effective surveillance mission plan.

E. Mutation Operator

The mutation operator is especially designed for this problem to enable area revisiting and take-off time scheduling. To illustrate the advantage of the custom mutation operator, the proposed EA is compared with the following two methods. Method-1 is an EA based on the proposed framework but without three custom mutation moves. In Method-2, which is based on the path planning method in [19], a single-period path is generated for each aircraft, and then this single-period path is copied to generate the multi-period path with the minimum downtime between two successive single-period paths. Note

0018-9251 (c) 2018 IEEE. Personal use is permitted, but republication/redistribution requires IEEE permission. See http://www.ieee.org/publications_standards/publications/rights/index.html for more information.

This article has been accepted for publication in a future issue of this journal, but has not been fully edited. Content may change prior to final publication. Citation information: DOI 10.1109/TAES.2018.2812538, IEEE Transactions on Aerospace and Electronic Systems

TABLE III: Results for the Problem using Different Methods

Method	f_1	f_2
The propose EA	**41.4**	**463.3**
Method-1	36.9	365.5
Method-2	22	330

TABLE IV: Results for the Problem When the Required Revisit Time is 4 Hours

Method	f_1	f_2	$-f_3$
The propose EA	**42.5**	445.3	**26.3**
Method-3	40	441.8	37.4
Method-4	41.4	**472.7**	107.8

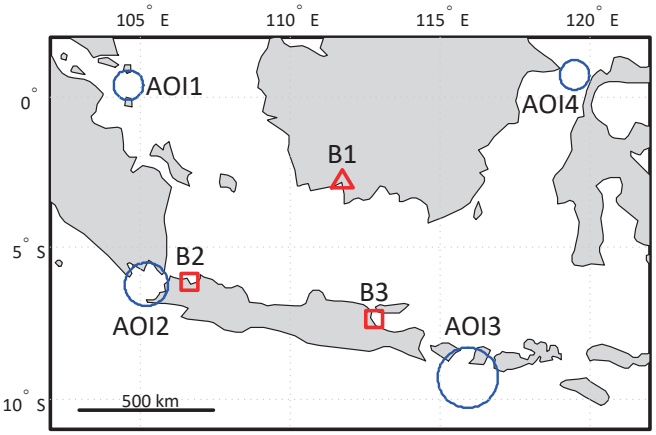

Fig. 8: The second simulation scenario: locations of AOIs and base stations.

that aircraft in the paths generated by Method-2 conducts a search in strips [19]; revisiting and take-off time scheduling are not enabled in Method-2.

Feasible solutions ($f_3 = 0$) are generated in these experiments. It can be seen from Table III that the proposed EA with custom mutation operator achieves the largest values of f_1 and f_2 comparing to the other two methods without problem-specific designs for revisiting and scheduling.

F. Revisit Violation Handling

Feasible solutions are generated when the requirement of revisit time is 8 hours. In this simulation, the mission scenario and configuration remain consistent with the previous ones, except the required revisit time changes to 4 hours. The proposed algorithm is compared with the following two methods. Method-3 is an EA based on the proposed framework but without *Reschedule* and without additional wait time at bases (aircraft land for the minimum downtime between successive flights). Method-4 is an EA based on the proposed framework but with the objectives $\max_P\ (f_1, f_2)$, in which the revisit constraint (20) is removed.

The sum of revisit violation time ($-f_3$) in the proposed EA is smaller than that in Method-3 mainly because the scheduling of take-off time by *Reschedule* enhances the temporal cooperation of aircraft so that the take-off time is adjusted to minimize $-f_3$ in the proposed algorithm. The comparison between the proposed EA and Method-3 illustrates the advantage of *Reschedule* designed in the mutation operator. Although the value of f_2 in Method-4 is the greatest among these three experiments, the revisit violation is much greater than that in the proposed EA. The proposed algorithm minimizes the sum of revisit violation time when there is no feasible solution w.r.t. constraint (20).

G. A Real-world Case Study

A more complex surveillance scenario that emerges from a real-world problem is set up, as shown in Fig. 8. Four water areas (circular areas in Fig. 8) are the AOIs. The radiuses of the AOIs are 55 km, 80 km, 110 km, and 55 km. Three aircraft are scheduled to perform a 48-hour mission. There is one type-1 aircraft and two type-2 aircraft. There is one base station (B1) for type-1 aircraft and two base stations (B2 and B3) for type-2 aircraft. Only one aircraft is assigned to one base station.

For type-1 aircraft, the maximum flight time is 10 hours, the minimum downtime is 2 hours and the maximum downtime is 3 hours. For type-2 aircraft, the maximum flight time is 5 hours, the minimum downtime is 1 hour and the maximum downtime is 1.5 hours. The speed of type-1 aircraft is 749 km/h and that of type-2 aircraft is 666 km/h. Each POI in an AOI must be revisited within 8 hours. Cells are circular areas with diameter 44 km. AOIs are segmented into 47 cells.

The parameters used in the proposed algorithm are the same as those in Section V-B. The population size is 1024. Feasible solutions ($f_3 = 0$) are generated for this mission scenario. The values of f_1 and f_2 in the best mission plan are 29.7 and 899.2, respectively. The path planning and scheduling takes 1242 seconds on average, based on the computer hardware described in the first simulation scenario. Note that this computation is done offline ahead of the missions.

VI. Conclusions

In this paper, a novel approach was described for the offline mission planning for multiple aerial vehicles to perform surveillance over disjoint areas. The formulation was presented for this multi-period coverage path planning and temporal scheduling problem, in which repeated visit of the same area in a path was considered. This revisiting feature is common in surveillance applications, but distinguishes the formulations and solution techniques of those in the vehicle routing problem and its variations. Objective functions were developed to promptly update information collected by covering AOIs and to ensure persistent surveillance. A multi-objective evolutionary algorithm with a novel chromosome representation and custom genetic operators, which enables the revisiting of areas and the scheduling of take-off time, was proposed. The proposed algorithm was computationally efficient even in large scale problems and can be ported to a variety of surveillance coverage problems.

0018-9251 (c) 2018 IEEE. Personal use is permitted, but republication/redistribution requires IEEE permission. See http://www.ieee.org/publications_standards/publications/rights/index.html for more information.

This article has been accepted for publication in a future issue of this journal, but has not been fully edited. Content may change prior to final publication. Citation information: DOI 10.1109/TAES.2018.2812538, IEEE Transactions on Aerospace and Electronic Systems

APPENDIX
NO-FLY ZONE AVOIDANCE

If there exist no-fly zones [9, 11] outside AOIs, they can be handled while generating single-period paths as follows. Vertices are added on the border or outside but close to the border of each no-fly zone. A penalty is defined for each edge in addition to the travel distance:

$$q_{ij} = \begin{cases} -M & \text{if the shortest path from vertex } i \text{ to} \\ & \text{vertex } j \text{ across no-fly zones} \\ 0 & \text{otherwise} \end{cases} \tag{38}$$

where M is a very large positive constant. The penalty for each edge is pre-computed based on whether the edge across no-fly zones or not. This penalty is included in the objective function of the single-period path planning:

$$\max_{x_{ij}} \quad \sum_{i \in S} \sum_{j \in V} \mathrm{sc}(i) x_{ij} + \sum_{i \in V} \sum_{j \in V} q_{ij} x_{ij} \tag{39}$$

Thus, aircraft can bypass no-fly zones in the single-period path. Once the single-period paths avoid no-fly zones, paths in the mission plan will avoid no-fly zones, because the genetic operators (Section IV-E) remove paths outside AOIs or add path segments inside AOIs, which will not cross no-fly zones.

REFERENCES

[1] T. Bektas, "The multiple traveling salesman problem: An overview of formulations and solution procedures," *Omega*, vol. 34, no. 3, pp. 209–219, 2006.

[2] N. Bostel, P. Dejax, P. Guez, and F. Tricoire, "Multi-period planning and routing on a rolling horizon for field force optimization logistics," in *The Vehicle Routing Problem: Latest Advances and New Challenges*, B. Golden, S. Raghavan, and E. Wasil, Eds. Boston, MA: Springer US, 2008, pp. 503–525.

[3] I.-M. Chao, B. L. Golden, and E. A. Wasil, "A fast and effective heuristic for the orienteering problem," *European Journal of Operational Research*, vol. 88, no. 3, pp. 475–489, 1996.

[4] H. Choset, "Coverage for robotics—A survey of recent results," *Annals of Mathematics and Artificial Intelligence*, vol. 31, no. 1–4, pp. 113–126, 2001.

[5] M. R. Chummun, Y. Bar-Shalom, and T. Kirubarajan, "Adaptive early-detection ML-PDA estimator for LO targets with EO sensors," *IEEE Transactions on Aerospace and Electronic Systems*, vol. 38, no. 2, pp. 694–707, Apr 2002.

[6] B. Crevier, J.-F. Cordeau, and G. Laporte, "The multi-depot vehicle routing problem with inter-depot routes," *European Journal of Operational Research*, vol. 176, no. 2, pp. 756–773, 2007.

[7] K. Deb and H. Jain, "An evolutionary many-objective optimization algorithm using reference-point-based non-dominated sorting approach, Part I: Solving problems with box constraints," *IEEE Transactions on Evolutionary Computation*, vol. 18, no. 4, pp. 577–601, Aug. 2014.

[8] K. Deb, A. Pratap, S. Agarwal, and T. Meyarivan, "A fast and elitist multiobjective genetic algorithm: NSGA-II," *IEEE Transactions on Evolutionary Computation*, vol. 6, no. 2, pp. 182–197, Apr. 2002.

[9] K. Doğançay, "UAV path planning for passive emitter localization," *IEEE Transactions on Aerospace and Electronic Systems*, vol. 48, no. 2, pp. 1150–1166, Apr. 2012.

[10] M. Drexl, "Rich vehicle routing in theory and practice," *Logistics Research*, vol. 5, no. 1–2, pp. 47–63, 2012.

[11] H. Ergezer and K. Leblebicioglu, "Path planning for UAVs for maximum information collection," *IEEE Transactions on Aerospace and Electronic Systems*, vol. 49, no. 1, pp. 502–520, Jan 2013.

[12] E. Galceran and M. Carreras, "A survey on coverage path planning for robotics," *Robotics and Autonomous Systems*, vol. 61, no. 12, pp. 1258–1276, 2013.

[13] F. Gavilan, R. Vazquez, and E. F. Camacho, "An iterative model predictive control algorithm for UAV guidance," *IEEE Transactions on Aerospace and Electronic Systems*, vol. 51, no. 3, pp. 2406–2419, July 2015.

[14] D. E. Goldberg, B. Korb, and K. Deb, "Messy genetic algorithms: Motivation, analysis, and first results," *Complex Systems*, vol. 3, pp. 493–530, 1989.

[15] J. H. Holland, *Adaptation in Natural and Artificial Systems: An Introductory Analysis with Applications to Biology, Control, and Artificial Intelligence*. MIT press, 1992.

[16] J. Hu, L. Xie, J. Xu, and Z. Xu, "Multi-agent cooperative target search," *Sensors*, vol. 14, no. 6, pp. 9408–9428, 2014.

[17] H. Jain and K. Deb, "An evolutionary many-objective optimization algorithm using reference-point based non-dominated sorting approach, Part II: Handling constraints and extending to an adaptive approach," *IEEE Transactions on Evolutionary Computation*, vol. 18, no. 4, pp. 602–622, Aug. 2014.

[18] P. J. Jones, "Cooperative area surveillance strategies using multiple unmanned systems," Ph.D. dissertation, School of Elect. & Comp. Eng., Georgia Tech, Atlanta, GA, 2009.

[19] O. Karasakal, "Minisum and maximin aerial surveillance over disjoint rectangles," *TOP*, vol. 24, no. 3, pp. 705–724, 2016.

[20] S. M. LaValle, *Planning Algorithms*. New York, NY, USA: Cambridge University Press, 2006.

[21] R. T. Marler and J. S. Arora, "The weighted sum method for multi-objective optimization: New insights," *Structural and Multidisciplinary Optimization*, vol. 41, no. 6, pp. 853–862, 2010.

[22] C. E. Miller, A. W. Tucker, and R. A. Zemlin, "Integer programming formulation of traveling salesman problems," *Journal of the ACM*, vol. 7, no. 4, pp. 326–329, Oct. 1960.

[23] A. Moitra, R. Mattheyses, V. DiDomizio, L. Hoebel, R. Szczerba, and B. Yamrom, "Multivehicle reconnaissance route and sensor planning," *IEEE Transactions on Aerospace and Electronic Systems*, vol. 39, no. 3, pp. 799–812, July 2003.

0018-9251 (c) 2018 IEEE. Personal use is permitted, but republication/redistribution requires IEEE permission. See http://www.ieee.org/publications_standards/publications/rights/index.html for more information.

This article has been accepted for publication in a future issue of this journal, but has not been fully edited. Content may change prior to final publication. Citation information: DOI 10.1109/TAES.2018.2812538, IEEE Transactions on Aerospace and Electronic Systems

[24] J. R. Montoya-Torres, J. L. Franco, S. N. Isaza, H. F. Jiménez, and N. Herazo-Padilla, "A literature review on the vehicle routing problem with multiple depots," *Computers & Industrial Engineering*, vol. 79, pp. 115–129, 2015.

[25] R. Pitre, X. Li, and R. Delbalzo, "UAV route planning for joint search and track missions—An information-value approach," *IEEE Transactions on Aerospace and Electronic Systems*, vol. 48, no. 3, pp. 2551–2565, July 2012.

[26] S. Ragi and E. K. P. Chong, "UAV path planning in a dynamic environment via partially observable Markov decision process," *IEEE Transactions on Aerospace and Electronic Systems*, vol. 49, no. 4, pp. 2397–2412, Oct. 2013.

[27] T. Sawik, "A note on the Miller-Tucker-Zemlin model for the asymmetric traveling salesman problem," *Bulletin of the Polish Academy of Sciences Technical Sciences*, vol. 64, no. 3, pp. 517–520, 2016.

[28] B. D. Song, J. Kim, and J. R. Morrison, "Rolling horizon path planning of an autonomous system of UAVs for persistent cooperative service: MILP formulation and efficient heuristics," *Journal of Intelligent & Robotic Systems*, vol. 84, no. 1, pp. 241–258, 2016.

[29] K. Tan, T. Lee, K. Ou, and L. Lee, "A messy genetic algorithm for the vehicle routing problem with time window constraints," *Proceedings of the 2001 Congress on Evolutionary Computation*, vol. 1, pp. 679–686, 2002.

[30] H. Tang and E. Miller-Hooks, "A tabu search heuristic for the team orienteering problem," *Computers & Operations Research*, vol. 32, no. 6, pp. 1379–1407, Jun. 2005.

[31] P. Toth and D. Vigo, Eds., *The Vehicle Routing Problem*. Philadelphia, PA, USA: Society for Industrial and Applied Mathematics, 2001.

[32] F. Tricoire, M. Romauch, K. F. Doerner, and R. F. Hartl, "Heuristics for the multi-period orienteering problem with multiple time windows," *Computers & Operations Research*, vol. 37, no. 2, pp. 351–367, 2010.

[33] G.-H. Tzeng and J.-J. Huang, *Multiple Attribute Decision Making: Methods and Applications*. Boca Raton, FL: CRC press, Taylor & Francis Group, 2011.

[34] P. Vansteenwegen, W. Souffriau, and D. V. Oudheusden, "The orienteering problem: A survey," *European Journal of Operational Research*, vol. 209, no. 1, pp. 1–10, 2011.

[35] T. Vidal, T. G. Crainic, M. Gendreau, N. Lahrichi, and W. Rei, "A hybrid genetic algorithm for multi-depot and periodic vehicle routing problems," *Operations Research*, vol. 60, no. 3, pp. 611–624, May 2012.

0018-9251 (c) 2018 IEEE. Personal use is permitted, but republication/redistribution requires IEEE permission. See http://www.ieee.org/publications_standards/publications/rights/index.html for more information.

DOCUMENT CONTROL DATA

*Security markings for the title, authors, abstract and keywords must be entered when the document is sensitive

1. ORIGINATOR (Name and address of the organization preparing the document. A DRDC Centre sponsoring a contractor's report, or tasking agency, is entered in Section 8.)

IEEE Transactions on Aerospace and Electronic Systems

2a. SECURITY MARKING (Overall security marking of the document including special supplemental markings if applicable.)

CAN UNCLASSIFIED

2b. CONTROLLED GOODS

NON-CONTROLLED GOODS
DMC A

3. TITLE (The document title and sub-title as indicated on the title page.)

Multi-period Coverage Path Planning and Scheduling for Airborne Surveillance

4. AUTHORS (Last name, followed by initials – ranks, titles, etc., not to be used)

Wang, Y.; Kirubarajan, T.; Tharmarasa, R.; Jassemi-Zargan, R.; Kashyap, N.

5. DATE OF PUBLICATION (Month and year of publication of document.)	6a. NO. OF PAGES (Total pages, including Annexes, excluding DCD, covering and verso pages.)	6b. NO. OF REFS (Total references cited.)
March 2018	15	35

7. DOCUMENT CATEGORY (e.g., Scientific Report, Contract Report, Scientific Letter.)

External Literature (P)

8. SPONSORING CENTRE (The name and address of the department project office or laboratory sponsoring the research and development.)

DRDC - Centre for Operational Research and Analysis
Defence Research and Development Canada
Carling Campus
60 Moodie Drive, building 7
Kanata ON K2H 8E9
Canada

9a. PROJECT OR GRANT NO. (If appropriate, the applicable research and development project or grant number under which the document was written. Please specify whether project or grant.)	9b. CONTRACT NO. (If appropriate, the applicable number under which the document was written.)

10a. DRDC PUBLICATION NUMBER (The official document number by which the document is identified by the originating activity. This number must be unique to this document.)	10b. OTHER DOCUMENT NO(s). (Any other numbers which may be assigned this document either by the originator or by the sponsor.)
DRDC-RDDC-2018-P106	

11a. FUTURE DISTRIBUTION WITHIN CANADA (Approval for further dissemination of the document. Security classification must also be considered.)

Public release

11b. FUTURE DISTRIBUTION OUTSIDE CANADA (Approval for further dissemination of the document. Security classification must also be considered.)

12. KEYWORDS, DESCRIPTORS or IDENTIFIERS (Use semi-colon as a delimiter.)

Path planning; sensor scheduling

13. ABSTRACT/RÉSUMÉ (When available in the document, the French version of the abstract must be included here.)

In this paper, optimal surveillance mission plans are developed to cover disjoint areas of interest (AOIs) over an extended time horizon using multiple aerial vehicles. AOIs to be covered are divided into a number of cells. To promptly update information collected from AOIs and to ensure persistent surveillance, each cell is to be revisited within a time slot. Joint path planning and temporal scheduling is formulated as a combinatorial optimization with the proposal of novel objective functions: 1) maximizing the minimum number of non-repeatedly covered cells in a sliding-window fashion and 2) maximizing the total number of covered cells in the mission plan. A multi-objective evolutionary algorithm (MOEA) with a specific chromosome representation and custom genetic operators, in which the constraint that each cell be revisited within a time slot is transformed into the third objective to handle infeasibility, is developed. The initial single-period paths are generated by solving a series of orienteering problems. The initial population is obtained by connecting these single-period paths and selecting the take-off time for each flight. Three mutation moves are proposed to enable revisiting in a single-period path and rescheduling of take-off time. The solutions converge in the MOEA and are selected by a weighted-sum model according to user preferences in decision making. Simulation results on different mission scenarios and different criteria show the superiority of the proposed algorithm. The algorithm is done offline ahead of the missions and requires modest computational resources.